HHS Public Access

Author manuscript

*J Comp Neurol*. Author manuscript; available in PMC 2021 September 29.

Published in final edited form as:

*J Comp Neurol*. 2009 February 01; 512(4): 453–466. doi:10.1002/cne.21895.

# Excitatory-Inhibitory Relationship in the Fascia Dentata in the Ts65Dn Mouse Model of Down Syndrome

**Pavel V. Belichenko**[1,*], **Alexander M. Kleschevnikov**[1], **Eliezer Masliah**[2], **Chengbiao Wu**[1], **Ryoko Takimoto-Kimura**[1], **Ahmad Salehi**[1], **William C. Mobley**[1]

[1]Department of Neurology & Neurological Sciences, the Center for Research and Treatment of Down Syndrome and Neuroscience Institute at Stanford University, Stanford University Medical Center, Stanford, California 94305-5489

[2]Departments of Neurosciences and Pathology University of California San Diego, School of Medicine, La Jolla, California 92093-0624

## Abstract

Down syndrome (DS) is a neurological disorder causing impaired learning and memory. Partial trisomy 16 mice (Ts65Dn) are a genetic model for DS. Previously, we demonstrated widespread alterations of pre- and postsynaptic elements and physiological abnormalities in Ts65Dn mice. The average diameter of presynaptic boutons and spines in the neocortex and hippocampus was enlarged. Failed induction of LTP due to excessive inhibition was observed. In this paper we investigate the morphological substrate for excessive inhibition in Ts65Dn. We used electron microscopy (EM) to characterize synapses, confocal microscopy to analyze colocalization of the general marker for synaptic vesicle protein with specific protein markers for inhibitory and excitatory synapses, and densitometry to characterize the distribution of receptor and several proteins essential for synaptic clustering of neurotransmitter receptors. EM analysis of synapses in the Ts65Dn vs. 2N showed that synaptic opposition lengths were significantly greater for symmetric synapses (~18%), but not for asymmetric ones. Overall, a significant increase in colocalization coefficients of GAD65/p38-immunoreactivity (IR) (~27%) and VGAT/p38-IR (~41%) was found, but not in VGLUT1/p38-IR. A significant overall decrease of IR in the hippocampus of Ts65Dn mice compared to 2N mice for glutamate receptor 2 (GluR2; ~13%), anti-γ-aminobutyrate amino acid $(GABA)_A$ receptor β2/3 subunit (~20%) was also found. The study of proteins essential for synaptic clustering of receptors revealed significant increase in puncta size for neuroligin 2 (~13%) and GABARAP (~13%), but not for neuroligin 1 and gephyrin. The results demonstrate a significant alteration of inhibitory synapses in fascia dentata of Ts65Dn mice.

### Indexing terms

Down syndrome; Ts65Dn; fascia dentata; synapses; receptors; inhibition; morphometry

[*]Correspondence to: Pavel V. Belichenko, Neuroscience Institute at Stanford University, Stanford University Medical Center, 1201 Welch Road, Room P220, Stanford, CA 94305-5489. pavel_belichenko@yahoo.com.

## Introduction

The balance between excitatory and inhibitory neurotransmission is essential for the normal function of neuronal circuits (Chen, 2004; Hensch and Fagiolini, 2005; Trevelyan and Watkinson, 2005; Akerman and Cline, 2007). A significant imbalance, whether of excitation or inhibition, is manifested as circuit dysfunction in a variety of episodic disorders, and may feature prominently in disorders due to acute or chronic injury or neurodegeneration. Imbalance of excitatory/inhibitory neurotransmission is linked to epilepsy, pain, parkinsonism, schizophrenia, bipolar disorder, autism, etc. (Benes and Berretta, 2001; Rubenstein and Merzenich, 2003; Rippon et al., 2007; Zold et al., 2007). Down syndrome (DS), due to trisomy chromosome 21, manifests in a variety of neurological abnormalities in both children and adults. Earlier work suggested that DS was characterized by an impaired balance between excitatory and inhibitory systems (Reynolds and Warner, 1988; Risser et al., 1997; but see Seidl et al., 2001). This has been supported by recent studies in mouse models of DS, in which increased inhibition in the hippocampus was shown to be responsible for failed induction of long-term potentiation (LTP) (Kleschevnikov et al., 2004). Measurements made in slice preparations of hippocampus indicate reduced synaptic plasticity through a marked reduction in LTP in the CA1 area (Siarey et al., 1997; Siarey et al., 1999; Galdzicki et al., 2001) of Ts65Dn mice and fascia dentata (FD) of Ts65Dn and Ts1Cje mice (Kleschevnikov et al., 2004; Belichenko et al., 2007). Rescue of apparently normal LTP by treating slices with picrotoxin, an inhibitor of $GABA_A$ receptors, pointed to an imbalance of neurotransmission manifested through increased inhibition. Raising the possibility that failed synaptic plasticity is linked to behavioral changes, Ts65Dn mice show spatial working and reference working memory impairments (Reeves et al., 1995; Demas et al., 1998; Escorihuela et al., 1998; Sago et al., 2000; Belichenko et al., 2007).

To explore further the molecular and cellular basis for increased inhibitory neurotransmission, we examined structural and biochemical features of synapses in the FD of Ts65Dn mice. We considered the following possibilities: inhibition was increased to a greater extent than excitation, inhibition was normal but excitation decreased, or both were decreased but with more marked changes in excitation. In view of earlier findings in FD, we favored the first alternative. Herein, we demonstrate that inhibition is selectively increased in Ts65Dn mice, as revealed by changes in ultrastructural, immunofluorescence and biochemical markers.

## Materials and Methods

### Mice husbandry

All experiments were conducted in accordance with the National Institutes of Health guidelines for the care and use of animals, and with an approved animal protocol from the Stanford University Institutional Animal Care and Use Committee. The Ts65Dn mouse colony was maintained for more than 10 generations by crossing B6EiC3Sn-Ts($17^{16}$)65Dn females (Jackson Laboratory, Bar Harbor, ME) with B6EiC3Sn F1/J A/a males (Jackson Laboratory). This breeding scheme was used because trisomic mice breed very poorly or not at all when inbred; the B6C3 background has been the most successful. To distinguish 2N from Ts65Dn mice, genomic DNA was extracted from tail samples. A quantitative PCR

protocol (provided by The Jackson laboratory) was used to measure *Mx1* gene expression, which is present in three copies in Ts65Dn. Male mice were used in all studies.

## EM processing and analysis

As previously described, ultrastructural analysis of synaptic architecture was performed on 6-month-old mice (Belichenko et al., 2004). In brief, mice were deeply anesthetized with sodium pentobarbital (200 mg/kg i.p.) (Abbott Laboratories, North Chicago, IL) and transcardially perfused with ice-cold 0.9% sodium chloride for 1 min, followed by ice-cold 4% paraformaldehyde and 1% glutaraldehyde in 0.1 cacodylate buffer, pH = 7.4, for 10 minutes. After perfusion, the brains were immediately removed and coronally sectioned (300-μm) on a vibratome and immersed in fixative. Sections were postfixed in 1% osmium tetroxide, stained with saturated uranyl acetate in 50% ethanol and then dehydrated through a graded series of ethanols to 90% ethanol; 2-hydroxypropyl methacrylate was the intermediate solvent. All infiltrations of 2-hydroxypropyl methacrylate and Scipoxy 812 resin (Energy Beam Sciences, Agawam, MA) were carried out on a shaker at slow speed. After two changes of 100% resin, the plates were polymerized in a 65°C oven for 24 hours. The plastic was detached, and selected areas were cut and glued onto dummy blocks. Thin sections (80 nm) were cut on a Reichert Ultracut E Ultramicrotome (Leica, Vienna, Austria), picked up onto 200-mesh copper grids (Electron Microscopy Sciences, Fort Washington, PA), and poststained in ethanolic uranyl acetate followed by bismuth nitrite (Electron Microscopy Sciences). Sections were analyzed with a Zeiss EM10 electron microscope (Zeiss, New York, NY). For morphometric analysis of synapses, 5 electron micrographs from each mouse were obtained at a final magnification of x10,000. The area of each image was 61 $\mu m^2$ and the total area studied for each animal was 305 $\mu m^2$ . Layer II-III of motor cortex and molecular layer of superior blade of FD were studied. The electron micrographs were digitized using Duoscan F40 (Agfa, Belgium). Using well established criteria for symmetric and asymmetric synapses (Gray, 1959; Kurt et al., 2000), we counted the number of each type of synapse on EM images. Synapses with prominent postsynaptic density were identified as asymmetric, while synapses with pre- and post-synaptic densities of equal thickness were considered as symmetric. Synapse length was defined as the length of the active zone. EM image was imported in “LazerPix” software (Bio Rad, UK) and line was draw along of each active zone using a mouse cursor and its length was measured.

## Indirect immunofluorescence

To study colocalization of synaptophysin (p38) with markers for inhibitory or excitatory synapses, slices were submitted to double labeling immunohistochemistry. In brief, 2N and Ts65Dn mice were deeply anesthetized with sodium pentobarbital (200 mg/kg i.p.) (Abbott Laboratories, North Chicago, IL) and transcardially perfused for 1 min with 0.9% sodium chloride (10 ml), then for 10 min with 4% paraformaldehyde in 0.1 M phosphate buffered saline (PBS), pH 7.4 (100 ml) for immunofluorescent methods. After perfusion, the brains were removed immediately and placed in the same fixative for 2-3 days. The brain was then sectioned coronally at 100-μm with a Vibratome (series 1000, TPI Inc., St. Louis, MO), and sections were placed in 0.1 M PBS. Free-floating coronal sections through the cortex and hippocampus from 3 month-old mice were pre-incubated in 5% non-fat milk in PBS, then incubated overnight at 4°C with mouse monoclonal anti-synaptophysin (i.e.,

p38; dilution 1:500) as the first primary antibody. The sections were then rinsed in PBS (20 min, 3 changes) and incubated for 1 h at room temperature with biotinylated goat anti-mouse IgG (1:200; Jackson ImmunoResearch Labs, West Grove, PA). After rinsing with PBS (20 min, 3 changes), sections were incubated with FITC-conjugated streptavidin (1:500; Jackson ImmunoResearch Labs, West Grove, PA) for 1 h at room temperature. After careful rinsing, the sections were incubated overnight at 4°C with one of the following second primary antibodies: rabbit anti-glutamic acid decarboxylase 65 (GAD 65; 1:1,000); rabbit anti-vesicular glutamate transporter 1 (VGLUT1; Bellocchio et al., 2000; dilution 1:1,000); rabbit anti-vesicular GABA transporter (VGAT; Chaudhry et al., 1998; dilution 1:1000). Sections were then rinsed in PBS (20 min, 3 changes) and incubated for 1 h at room temperature with Texas red-conjugated donkey anti-rabbit secondary antibody (1:200; Jackson ImmunoResearch Labs, West Grove, PA). Following further careful rinsing, the sections were mounted on microscope glass slides and coverslipped with 90% glycerol in PB.

For single antibody labeling, sections from 2N and Ts65Dn mice were pre-incubated in 5% non-fat milk in PBS, then incubated overnight at 4°C with the primary antibody. The sections were rinsed in PBS (20 min, 3 changes) and incubated for 1 h at room temperature with species-appropriate biotinylated secondary antibodies (1:200; Jackson ImmunoResearch Labs, West Grove, PA). After rinsing with PBS (20 min, 3 changes), sections were incubated with FITC-conjugated streptavidin (1:500; Jackson ImmunoResearch Labs, West Grove, PA) for 1 h at room temperature. Following further careful rinsing, the sections were mounted on microscope glass slides and coverslipped with 90% glycerol in PB. Optimal antibody concentrations were determined for each antibody; in control experiments, omitting primary antibodies eliminated immunoreactivity.

## Antibody characterization

The following text and Table 1 provide information on all antibodies used in this manuscript. All antibodies have previously been characterized by Western blot analysis and immunohistochemistry and are commercially available. The synaptophysin (i.e., p38; dilution 1:500) antibody recognized a single band at ~38 kDa on Western blot of rat brain lysate; immunoadsorption of this antibody with a 0.1% Triton X-100 extract from purified rat brain presynaptic vesicles gave negative results. The glutamic acid decarboxylase 65 (GAD65; dilution 1:1,000) antibody was purchased from Chemicon. According to the manufacturer's product information, this antibody reacts strongly with GAD65-containing nerve terminals and recognizes a 65 kDa protein corresponding GAD65 by Western blot of mouse brain extract. The vesicular GABA transporter (VGAT; Chaudhry et al., 1998; dilution 1:1,1000) antibody was produced by immunizing rabbits with a GST fusion protein containing N-terminal 99 amino acids of rat VGAT (see more details in Chaudhry et al., 1998). On Western blots of brain extracts from rat brain this antibody recognized a single 55-60 kDa band in agreement with the molecular weight calculated from the amino acid composition. There was no staining of liver or control PC12 cells under the same conditions; however, VGAT-expressing PC12 cells show a band with similar molecular mass. The vesicular glutamate transporter 1 (VGLUT1; Bellocchio et al., 2000; dilution 1:1,000) antibody was produced by immunizing rabbits with a GST fusion protein containing the last

68 amino acids (residues 493–560) of rat brain-specific $Na^+$-dependent inorganic phosphate transporter (see more details in Bellocchio et al., 2000); preadsorption of this antibody with the GST fusion protein used as the immunogen completely abolishes immunoreactivity in brain sections. The glutamate receptor 2 (GluR2; dilution 1:500) antibody on Western blots of brain extracts from mice recognizes a ~102 kDa band corresponding to full length GluR2; another ~66 kDa band appear to be a breakdown product of GluR2. Preincubation of brain sections with the fusion protein GluR2 entirely blocked the immunoreactivity of this antibody. The glutamate receptor 1 (GluR1; dilution 1:1000) antibody had no cross-reaction with GluR2-4. According to the manufacturer's product information, Western blot analysis of rat brain extracts shows a single band co-migrating with GluR1 (105-107 kDa) expressed in transfected cells. Our data on mouse brain extract also showed a single 105-107 kDa band (Table S2). Specificity of this antibody was proven by using Western blot analysis of membranes from COS-7 cells transfected with the GluR1 cDNAs. Specific staining by this antibody on a Western blot of the soluble fraction from rat brain membranes was completely eliminated by preincubation of the antibody with the immunizing peptide. The $GABA_A$ receptor β2/3 subunit (dilution 1:500) antibody was purchased from Upstate. According to the manufacturer's product information, this antibody was directed against affinity-purified $GABA_A$ receptor isolated from bovine brain. Western blot of rat brain microsomal preparations showed a 55 kDa band for β2 and a 57 kDa band for β3 subunits. Our data on mouse brain extract also showed identical bands (Table S2). The $GABA_A$ receptor α1 subunit (dilution 1:500) antibody recognized a single band of 51 kDa for α1 subunit on Western blot of rat brain microsomal preparations (manufacturer's datasheet) and our data on mouse brain extract showed an identical band (Table S2). The $GABA_B$ receptor R1 subunit (dilution 1:100) antibody recognized a band of ~130 kDa corresponding to the molecular weight for the biggest splice variant $GABA_B$ receptor R1a subunit on Western blot of rat brain membrane preparation. Mouse brain extract showed an identical band (Table S2). As a control, primary antibody that was preabsorbed with their peptide antigen gave no specific staining. The $GABA_B$ receptor R2 subunit (dilution 1:100) antibody recognized a single band of ~105 kDa by Western blot of whole rat brain membrane preparations (manufacturer's datasheet) and our data on mouse brain extract showed an identical band (Table S2). Using this antibody, we observed a staining pattern of immunofluorescent distribution in the mouse hippocampus that was identical with a previous report (Fritschy et al., 1999). The neuroligin (clone 4F9, dilution 1:1,000) antibody recognizes mouse neuroligins 1, 2 and 3 as determined by Western blotting of cell lysates from HEK293 cells transfected with neuroligin 1, 2 or 3 cDNAs. Transfecting of hippocampal neurons in culture with lentiviruses delivering small-hairpin RNA (shRNA) for individual neuroligin isoforms reduced neuroligin expression in an isoform specific manner; co-infection with shRNAs for all three neuroligin isoforms, completely abolished staining on Western blot. The neuroligin 1 (clone 4C12, dilution 1:1,000) antibody recognizes mouse neuroligin 1, no cross reactivity was observed with neuroligin 2 or with neuroligin 3 (manufacture's datasheet). Transfection of hippocampal neurons in culture with lentiviruses delivering shRNA for neuroligin 1 reduced neuroligin 1 expression on Western blot. The neuroligin 2 (dilution 1:1,000) antibody recognizes a 93 kDa band on Western blot of EOC 20 whole cell lysates (manufacturer's datasheet) and our data on mouse brain extract showed an identical band (Table S2). Transfection of hippocampal neurons in culture with lentiviruses delivering

shRNA for neuroligin 2 reduced neuroligin 2 expression with >90% efficiency in single cells and was confirmed by the absence of immunostaining when using this antibody. The GABARAP (dilution 1:500) antibody recognizes a single 14 kDa band on Western blot of human brain lysate (manufacturer's datasheet). Tranfection of hippocampal neuronal cultures with small interfering RNA against GABARAP significantly reduced dendritic GABARAP fluorescence intensity (Marsden et al., 2007). The gephyrin (clone mAb7a, dilution 1:500) antibody recognizes mouse, rat, human, pig, and goldfish gephyrin. This antibody detects only the brain-specific 93 kDa splice variant on crude synaptic membrane fractions of rat brain (manufacturer's datasheet), and displayed a staining pattern and distribution in the mouse hippocampus that was identical with previous report (Kralic et al., 2006).

## Confocal microscopy

Confocal imaging of brain slices labeled with one or two fluorophores was performed as previously described (Belichenko et al., 2004). Sections were scanned in a Radiance 2000 confocal microscope (BioRad, Hertfordshire, United Kingdom) using a Nikon Eclipse E800 fluorescence microscope. The laser was an argon/krypton mixed gas laser with exciting wavelengths for FITC (488 λ) and for Texas Red (568 λ). The optimal condition for confocal imaging of single immunoreactivity (IR) was the following: the lens was a x20 objective (Nikon; Plan Apo x20/0.75); LaserSharp 2000 (Bio Rad) software was used; laser power was 10%; the zoom factor was 3; 500 fast speed scanning was employed. Each optical section was the result of 3 scans by Kalman filtering, the size of the image was 512 × 512 pixels (i.e., 246 × 246 μm). Dual-channel confocal microscopy was employed to study colocalization of p38-IR with markers for inhibitory or excitatory synapses. The optimal conditions for this method were: the lens was a x60 objective (Plan Apo 60x/1.40 oil); LaserSharp 2000 (Bio Rad) software was used; laser power was 10% for “green” and 50% for “red” channels; the zoom factor was 6; scanning was at 500 lps; a sequential mode of scanning was employed to reduced “bleed through”; each optical section was the result of three scans with Kalman filtering; image size was 512 × 512 pixels (i.e., 34 × 34 μm).

## Image acquisition and analysis

For quantitative analysis of p38-IR and VGLUT, GAD65 or VGAD-IR colocalization “LazerPix colocalization” software (Bio Rad, UK) was used. Two slices per mouse were used; 20 images from the both the left and right side for each mouse (with n = 3, for a total 60 values) were analyzed. For each image, the intensity thresholds were estimated by analyzing the distribution of pixel intensities in the image areas that did not contain IR. This value, the background threshold, was then subtracted and red-green colocalization coefficients were calculated.

Quantitative analysis of IR for neurotransmitter receptors and for synaptic proteins was carried out on single optical images using Scion software (Scion Corporation, Frederick, Maryland, USA). Two slices per mouse were used; 6 images from the left and right side from each mouse (with n = 6, for a total 36 values) were analyzed. For every area, background fluorescence was estimated on sections incubated without primary antibody (i.e. the optical density (OD) background). This value was then subtracted

from the corresponding section stained with primary antibody to obtain the OD of immunofluorescence.

### Gene expression and western blot studies

Real time PCR and western blot were applied to measure gene expression and protein levels in the hippocampus (see details in Supplemental Material and Methods). For gene expression studies, five 2N and 5 Ts65Dn mice of age 3 months were used, as described in Supplemental Material and Methods. For western blot, six 2N and 5 Ts65Dn mice 4 months old were used, as described in Supplemental Material and Methods.

### Statistical analyses

The data for synapse number and size, colocalization of p38-IR with markers for inhibitory or excitatory synapses, gene expression, protein measurement by western blot, and receptor and synaptic proteins were exported to Excel (Microsoft, Redmond, WA), and statistical comparisons were performed using two-way analysis of variance (ANOVA) and for two samples using two-tailed Student's *t*-test. All results are expressed as mean ± SEM, and $P$ values < 0.05 were considered significant.

## Results

We analyzed the morphology of excitatory and inhibitory synapses using several approaches: i) EM for morphometry of asymmetric and symmetric synapses; ii) double immunofluorescence for quantitative analysis of coefficient of colocalization; and iii) densitometry of immunofluoresecence for quantitative analysis of receptor distributions, and the number and size of receptor clusters.

### Selective changes in the ultrastructure of symmetric synapses in the Ts65Dn FD

Using established criteria for defining symmetric and asymmetric synapses (Gray, 1959; Kurt et al., 2000), we counted the number of each type of synapse on EM images (Fig. 1a,b). In the FD, the total density of synapses was not significantly different between 2N and Ts65Dn mice (Fig. 1c; $P = 0.77$). Also, there was no significant difference in the ratio of asymmetric/symmetric synapses (Fig. 1d; $P = 0.34$). However, the average synaptic apposition length of synapses was significantly greater in Ts65Dn vs. 2N mice (Fig. 1e; $P < 0.001$. Most interesting was the finding that the synaptic apposition lengths were significantly greater for symmetric ($P < 0.001$), but not for asymmetric synapses ($P = 0.99$). The change appears to affect the entire population of symmetric synapses. The frequency distribution histogram shows a shift to larger sizes of the entire population of symmetric synapses, with no change in the distribution of assymetrical synapses (Fig. 1f). These findings are evidence for neurotransmitter-selective changes in synaptic structure in the Ts65Dn FD.

### Increased colocalization of p38-IR with markers for inhibitory synapses in the Ts65Dn FD

To characterize further excitatory-inhibitory relationships in FD, we used double labeling immunofluorescence with anti-p38 antibody, to mark all synapses, and with markers for excitatory (anti-VGLUT1 antibody) or inhibitory synapses (anti-GAD-65 or anti-vGAT

antibodies). Comparing 2N and Ts65Dn mice, and focusing first on p38-IR, the density of individual puncta of p38-IR was unchanged overall (2N: 2.01 ± 0.11 puncta/μm$^2$, Ts65Dn: 2.04 ± 0.08 puncta/μm$^2$, n = 3; $P = 0.84$). However, in FD of Ts65Dn mice the area occupied by p38-IR increased significantly by an average of 28% ($P = 0.01$) and the size of p38-IR puncta increased by an average of 21% (2N: 0.067 ± 0.007 μm$^2$, Ts65Dn: 0.081 ± 0.002 μm$^2$, n = 3; $P = 0.04$).

To test the idea that the change in p38-IR in the Ts65Dn FD was due to selective changes in inhibitory synapses, we extended the quantitative analysis to examine colocalization of p38-IR with markers for excitatory or inhibitory synapses. There was no difference in the average colocalization coefficient for VGLUT1-IR/p38-IR (2N: 0.72 ± 0.02, Ts65Dn: 0.79 ± 0.03, n = 3; $P = 0.09$). The density of individual puncta of VGLUT1-IR was overall the same in FD (2N: 2.05 ± 0.08 puncta/μm$^2$, Ts65Dn: 1.98 ± 0.07 puncta/μm$^2$, n = 3; $P = 0.55$). These findings provided no evidence for changes in the size of excitatory synapses in the FD of Ts65Dn mice.

A different picture emerged in the quantitative analysis of p38-IR with inhibitory markers. The coefficient of colocalization in the molecular layer showed a significant overall increase in GAD65-IR/p38-IR (Fig. 2; $P = 0.01$). The density of individual GAD65-IR puncta did not differ (2N: 1.05 ± 0.08 puncta/μm$^2$, Ts65Dn: 1.13 ± 0.06 puncta/μm$^2$, n = 3; $P = 0.44$). Similarly, examining p38-IR and vGAT-IR colocalization, the coefficient of colocalization in the molecular layer of FD showed a significant overall increase in vGAT-IR/p38-IR in Ts65Dn (2N: 0.22 ± 0.02, Ts65Dn: 0.31 ± 0.01, n = 3; $P < 0.01$). Finally, the density of individual vGAT-IR puncta did not differ (2N: 1.89 ± 0.07 puncta/μm$^2$, Ts65Dn: 1.74 ± 0.14 puncta/μm$^2$, n = 3; $P = 0.36$). We conclude that the increase in colocalization with p38-IR of GAD65-IR and vGAT-IR, but not with VGLUT1-IR, reflects a change in inhibitory synapses in the FD of Ts65Dn mice. They are further evidence for a neurotransmitter system-selective change.

## Gene expression and immunoblotting studies of receptors and synaptic proteins

Changes in the structure of inhibitory synapses predicted changes in the expression of genes for neurotransmitter receptors and synaptic proteins that mediate inhibitory neurotransmission. We examined inhibitory and excitatory receptors and functionally-related peptides in sections from the hippocampus in 2N and Ts65Dn mice. As measured at the mRNA level, the expression of the genes for $GABA_A$ receptors (subunits β2, β/3 and α1) and $GABA_B$ receptors (subunits R2 and R1) did not differ (Table S1). We also detected no changes in the mRNA levels for the excitatory neurotransmitter receptors GluR1 and GluR2 (Table S1). Four proteins essential for synaptic clustering of neurotransmitter receptors were also studied. Neuroligin 1 is present at excitatory synapses where, as a cell adhesion protein, it plays a role in postsynaptic formation and remodeling (Chih et al., 2005). At inhibitory synapses, neuroligin 2 appears to play the same or a similar role (Chih et al., 2005). Gephyrin is a microtubule-associated bridging protein for inhibitory glycine receptors (Meier and Grantyn, 2004). GABARAP is $GABA_A$ receptor associated protein that interacts with the γ2 subunit of $GABA_A$ receptors (Wang and Olsen, 2000). We detected no change in the expression of any of these genes at the mRNA level (Table S1).

Next, we asked if changes could be detected at the protein level. Hippocampal lysates from 2N and Ts65Dn mice were examined by immunoblotting. Loading equal amounts of total protein, no significant differences were detected (Table S2). These findings provided no evidence for marked changes in overall levels of several gene products that mediate excitatory and inhibitory neurotransmission in Ts65Dn hippocampus.

## Immunolocalization of neurotransmitter receptors and synaptic proteins in the hippocampus

Because studies of gene expression examined the entire hippocampus, we reasoned that changes in specific regions of the hippocampus may have gone undetected. To study differences in the regional distribution of receptors, we used single labeling immunofluorescence for markers of excitatory glutamate receptors (anti-GluR1 and anti-GluR2 antibody) or inhibitory synapses (anti-$GABA_A$ receptors subunits β2/3 or α1 and $GABA_B$ receptors subunits R2 or R1 antibodies) and quantified IR using confocal microscopy. The same strategy was used to examine the distribution of the synaptic proteins gephyrin, GABARAP and neuroligins 1 and 2 in the molecular layer of FD at age 6 to 7 months (Figs. 4, 5).

**Glutamate Receptors—**We investigated the distribution of glutamate receptors (GluR1 and GluR2) in both blades of the dentate gyrus and in CA1 of Ts65Dn and 2N mice. There was a significant overall reduction of GluR2 immunostaining (Fig. 3a,b) in Ts65Dn mice age 3 months (Table 2). Reductions were found in FD (granular cell layer, inferior blade and inner and middle molecular layers of superior blade), hilus and stratum lacunosum moleculare (Table 2). In Ts65Dn mice at age 8 months, the differences in GluR2 receptor IR reached significance in the superior blade of FD and in the stratum lacunosum moleculare layer of CA1 (Table 2). Comparing the two ages, the changes in the superior blade and CA1 were more marked in older mice.

Significant reduction of GluR1 receptor IR was detected in the outer molecular layer of the inferior blade and stratum lacunosum molecular of Ts65Dn mice age 3 months, and in hilus and stratum lacunosum molecular of these mice age 8 months (Table 2). However, most values for GluR1 receptor IR in Ts65Dn mice were not significantly different from 2N mice at either 3 or 8 months (Table 2). Nor could we detect an apparent change in the intensity of IR between 3 and 8 months.

Examining the ratio of immunostaining for GluR2/GluR1, significant negative deviations from 1.0 were detected in the outer molecular layer of inferior blade at 3 months, in the molecular layer of the superior blade and in stratum radiatum of CA1 at 3 month; a significantly increased ratio was detected for the hilus at 8 months.

**$GABA_A$ Receptors—**We investigated the distribution of $GABA_A$ receptors (subunits β2/3 and α1) in Ts65Dn and 2N mice ages 3 and 8 months (Table 3). At age 3 months, the overall IR of $GABA_A$ subunits β2/3 was reduced in Ts65Dn mice (Fig. 3c,d); decreases reached significance in all regions of the inferior blade of FD, in the inner molecular layer of the superior blade of FD, in the hilus, and in all strata of CA1 (Table 3). In contrast, we detected no significant changes in amount of β2/3 at age 8 months. While the lack of significant

changes at this age relative to 2N mice can be ascribed in part to increased variability of the measurements, the most salient change was a marked increase in the overall level of IR (Table 3). Indeed, the overall IR of $GABA_A$ β2/3 in Ts65Dn was elevated from 80% at 3 months to 99% at 8 months vs. 2N ($P < 0.01$). Thus, IR for β2/3 subunits appears to have increased considerably between 3 and 8 months (Table 3).

IR for $GABA_A$ α1 subunits showed little change relative to 2N mice; it was significantly reduced only in stratum lacunosum moleculare and only at 3 months (Table 3). The ratio of $GABA_A$ β2/3 to α1 was calculated to attempt to evaluate subunit composition (Table 3). The values deviated significantly from 1.0 as follows: at 3 months of age: 20-30% less in molecular layer of inferior blade FD, ~28% less in granular layers, 14% less in inner and outer molecular layer of superior blade FD, and 24% less in pyramidal layer of CA1; at age 8 months: 16% less in outer molecular layer of superior blade FD and 24% more in pyramidal layer of CA1. More interesting was the finding that, because of the relative increase in IR for β2/3 subunits, the overall average ratio was increased from 0.83 at 3 months to 1.01 at 8 months, a difference that was significant ($P < 0.01$). We conclude that there are age-related changes in immunostaining for $GABA_A$ receptors in the hippocampus of Ts65Dn mice.

**$GABA_B$ Receptors—**We also investigated the distribution of IR for $GABA_B$ receptors (subunits R2 and R1) in Ts65Dn and 2N mice ages 3 and 11.5 months (Table 4). At age 3 months, the overall IR for R1 or R2 subunits was unchanged in Ts65Dn mice, except in the granular layers of FD (14% less $GABA_B$ R1; $P = 0.02$) (Table 4). In contrast, significantly less $GABA_B$ R1 immunostaining was found in Ts65Dn mice age 11.5 months in the superior blade of FD, in hilus, and in CA1 (Table 4). $GABA_B$ receptor R2 subunit was unchanged at 11.5 months of age (Table 4). The ratio of $GABA_B$ R1 to R2 was not significantly different from 1.0 at 3 months, but at 11.5 months was decreased by ~ 14% in FD, 30% in hilus, and 20% in CA1. As for $GABA_A$ receptors, these findings are evidence for changes in $GABA_B$ receptors during aging, but with an overall decrease rather than the increase documented for $GABA_A$ receptors.

Next we studied the distribution of proteins essential for synaptic clustering of neurotransmitter receptors: gephyrin, GABARAP and neuroligins in 2N and Ts65Dn mice age 6 to 7 months (Figs. 4, 5).

**Gephyrin—**Examining immunostaining for this protein, we evaluated the density of puncta, the size of puncta and the average OD of puncta. There was no difference in the average density of gephyrin-IR puncta in Ts65Dn vs. 2N (Fig. 4a-c; $P = 0.94$). The average size of gephyrin-IR puncta in Ts65Dn vs. 2N was also the same (Fig. 4d; $P = 0.22$). The average OD of puncta was correspondingly unchanged (2N: 123.58 ± 0.42, Ts65Dn: 123.00 ± 043, n = 6; $P = 0.34$).

**GABARAP—**There was significant difference (increase of 33%) in the average density of GABARAP-IR puncta in Ts65Dn vs. 2N (Fig. 4e-g; $P = 0.01$). The average size of individual GABARAP-IR puncta in Ts65Dn vs. 2N was also significantly greater (increase of 15%) (Fig. 4h; $P = 0.01$).

**Neuroligins—**Using an antibody (clone 4F9) that marks both neuroligin 1 and 2, we detected no difference in the average density of neuroligin-IR of individual puncta in Ts65Dn vs. 2N (Fig. 5a-c; $P = 0.06$). However, the average size of individual neuroligins-IR puncta was significantly larger in the Ts65Dn by 14% (Fig. 5d; $P < 0.01$).

There was no difference in the average density of neuroligin 1-IR (clone 4C12) individual puncta numbers in Ts65Dn vs. 2N (Fig. 5e-g; $P = 0.25$). The average size of individual neuroligin 1-IR puncta in Ts65Dn vs. 2N was also the same (Fig. 5h; $P = 0.17$).

However, there was a significant difference (55% increase) in the average density of neuroligin 2-IR individual puncta numbers in the Ts65Dn (Fig. 5i-k; $P = 0.02$). In addition, the average size of individual neuroligin 2-IR puncta in Ts65Dn was significantly greater (13%) (Fig. 5l; $P = 0.03$). These data are further evidence for changes in inhibitory synapses in the Ts65Dn hippocampus.

### Ultrastructural studies of motor cortex

In earlier studies, we noted that changes in the size of presynaptic boutons and spines involved not just hippocampus but other regions as well, including motor cortex (Belichenko et al., 2004). To discern whether or not the ultrastructural changes in hippocampus extended to other affected regions, we examined using EM the motor cortex of Ts65Dn and 2N mice. As for the hippocampus, the total density of synapses was not significantly different between 2N and Ts65Dn mice (Fig. S1; $P = 0.83$). There was also no significant difference in the ratio of asymmetric/symmetric synapses in the motor cortex (Fig. S1; $P = 0.77$). The average length of synaptic appositions was increased in motor cortex (Fig. S1; $P < 0.01$). In contrast to the findings in hippocampus, synaptic apposition lengths in motor cortex were significantly greater for asymmetric synapses (Fig. S1; $P < 0.01$), but not for symmetric synapses (Fig. S1; $P = 0.39$). Thus, while synaptic structures show widespread changes, detailed examination shows that brain regions differ in the type of changes detected.

## Discussion

Our study provides evidence for selective involvement of inhibitory neurotransmission in the FD of the Ts65Dn mouse. Extending recent physiological studies documenting increased inhibition, the current report shows that these changes are linked to marked changes in the structure of synapses. Comparing Ts65Dn mice with their 2N controls, we detected: a selective enlargement of the active zones of asymmetric synapses, increased colocalization of p38 with markers for inhibitory neurotransmission, and increased immunostaining for synaptic proteins that mark inhibitory synapses. Remarkably, the changes in FD appear to be region-specific, because a very different pattern of changes was seen in the motor cortex. The findings for hippocampus suggest that changes in inhibitory neurotransmission are progressive, raising the possibility that they are compensatory to undefined cellular events. In providing new insight to the neurobiology of DS, this work points to the importance of defining more fully the excitatory and inhibitory circuits of the DS hippocampus and continuing studies to restore the balance of excitatory and inhibitory neurotransmission.

### Selective changes in inhibitory synapses in FD of Ts65Dn mice

Quantitative analysis of EM data revealed no significant difference in the area density of synapses of all types combined and asymmetric/symmetric ratio of synapses in FD and motor cortex of Ts65Dn vs. 2N mice. The findings are consistent with those of Kurt and colleagues (2000) who found no significant difference in the area density when all synapses were included. Also, Kurt and colleagues (2000), and an earlier (Belichenko et al., 2004) and current study from this laboratory, showed a significantly greater synaptic apposition zone length in Ts65Dn vs. 2N mice that extended to both symmetric and asymmetric synapses. In contrast to our findings, while Kurt and colleagues (2000) detected a significant reduction of asymmetric synapses in the temporal cortex of aged mice, we found no evidence for synaptic loss in young mice. Furthermore, we found that synaptic length of symmetric synapses was selectively increased in FD and that the reverse was true in motor cortex. It is now apparent that region-specific differences exist with respect to the type of synapses whose size is increased: symmetric synapses in FD, asymmetric synapses in motor cortex, and both in temporal cortex (Kurt et al., 2000).

To confirm that inhibitory synapses were those identified in the EM studies, we employed double labeling immunohistochemistry to study colocalization of p38 with markers for inhibitory or excitatory synapses. The antibody against p38 labeled all synapses, while antibodies against GAD65 or vGAT labeled only inhibitory and the antibody against VGLUT1 marked only excitatory synapses. In studies of colocalization of these markers, we detected an overall significant increase in colocalization coefficients for GAD65 with p38-IR (~27%) and for VGAT with p38-IR (~41%); in contrast, there was no increase in the colocalization for VGLUT1 with p38-IR. Taken together, the morphological studies point compellingly to changes in inhibitory synapses that are significant and selective in FD of Ts65Dn mice.

### Changes in inhibitory synaptic proteins in FD of Ts65Dn mice

The results of morphological studies suggested that selective changes might also be detected in the synaptic proteins and receptors that mediate inhibitory neurotransmission. Using confocal microscopy, we noted changes in the distributions of proteins essential for receptor clustering in the Ts65Dn hippocampus. There was a significant increase in the size and number of IR puncta for neuroligin 2 and GABARAP (both by ~13%), proteins that mark inhibitory synapses (Wang and Olsen, 2000; Chih et al., 2005), but not for neuroligin 1, which marks excitatory synapses (Chih et al., 2005). Though the changes in immunostaining for neuroligin 2 and GABARAP were robust, they were not detected by immunoblotting. The most plausible explanation is that the changes were diluted by examining the entire hippocampus. Of note, there is no change in gephyrin, a microtubule-associated bridging protein of glycine receptors (Meier and Grantyn, 2004), in Ts65Dn mice, suggesting that changes in inhibitory synapses select a subset of proteins and receptors. These data are further evidence for significant changes in inhibitory synapses.

### Changes in both excitatory and inhibitory receptors in Ts65Dn mice

Keys to the operation of synapses are the receptors for glutamate and GABA. Therefore, we examined next receptors that mediate excitatory and inhibitory neurotransmitter systems

at the protein level, using immunoblotting and confocal immunofluorescence microscopy. The latter studies contributed the most salient findings. We examined the hippocampal region-specific distributions of receptor IR using antibodies against GluR1, GluR2, $GABA_A$ receptor α1 and β2/3 subunits, and $GABA_B$ receptors R1 or R2 subunits. Significant changes were detected for GluR2, $GABA_A$ β2/3 and $GABA_B$ R1, with differences noted between the ages examined (Tables 2-4). There was an overall decrease of IR in the hippocampus in young Ts65Dn mice for GluR2 (~13%) and for $GABA_A$ receptor β2/3 subunit (~20%). Older Ts65Dn mice showed an overall decrease in IR for GluR2 (~18%) and $GABA_B$ receptor R1 (~19%). Perhaps the most interesting findings were for changes in the relative amounts with respect to 2N mice between the ages examined. The pattern was for decreases in GluR2 and $GABA_B$ R1 subunits inversely correlate with increases in $GABA_A$ β2/3. These data are evidence against the view that changes in inhibitory neurotransmission, or indeed of inhibitory synapses, can be explained simply by an increase in the number of inhibitory receptors or a decrease in excitatory receptors. Instead, it will be necessary to explore in detail and quantitatively, including at the protein level, the precise loci of the changes detected within hippocampal networks in which increased inhibition has been demonstrated.

## Understanding the neurobiology of synaptic changes in the Ts65Dn hippocampus

The balance between excitation and inhibition, and the plasticity of circuits, is partly a function of the number of such receptors, their subunit composition, and the cellular elements in which they are expressed. Deviations from normal can readily be envisioned, and have been shown, to contribute to neurological disorders (Luscher and Keller, 2004; Greger et al., 2007). In Ts65Dn mice, on average the GluR2/GluR1 ratio was 0.99 ± 0.02 in hippocampus for young and 0.95 ± 0.03 for old mice. However, there was a 13% decrease in the outer molecular layer of the inferior blade for young Ts65Dn mice. As mice aged, the GluR2/GluR1 ratio decreased by 13-26% in all three sublayers of molecular layer in superior blade, as well as in the stratum radiatum of CA1. In contrast, a 13% increase was noted in hilus. The physiological consequence of such changes is as yet obscure, but the speculation can be offered that synaptic plasticity may be decreased to a greater extent with aging in the Ts65Dn hippocampus. The decrease in the levels of GluR2 receptors, whose presence within AMPA receptors regulates calcium flux (Isaac et al., 2007), may contribute to the demonstrated alterations in synaptic plasticity in Ts65Dn mice (Siarey et al., 1997; Galdzicki et al., 2001; Kleschevnikov et al., 2004).

Perhaps consistent with a decrease in synaptic plasticity are the changes detected in $GABA_A$ and $GABA_B$ receptors during aging. Here there was a relative increase in $GABA_A$ receptor β2/3 subunits with aging and an increase in the ratio of β2/3 to α1 subunit of 18%. Although, the physiological consequences of such alterations are uncertain, these changes may reflect a compensatory adjustment of the inhibitory circuits during the lifespan. If so, the question arises what stimulus could be responsible. It will be important to consider in future studies the possibility of a preexisting and persistent increase in excitatory neurotransmission that induces a compensatory change in inhibitory neurotransmission and to test the idea rigorously through electrophysiological studies in very young mice. Studies to examine in detail the structure and function of inhibitory synapses will also be essential.

Using this approach it will be possible to understand the underlying pathophysiology of circuits and the methods that might be used to enhance hippocampal function.

### Similarity in alterations of excitatory-inhibitory relationship in subjects with DS and Ts65Dn mice

Most of the neuropathological literature for DS subjects has focused on cholinergic neurotransmitter systems (Casanova et al., 1985; Mann et al., 1985; see also review in Salehi et al., 2007). Few studies address amino acid neurotransmitters and the circuits in which they participate and the findings are as yet inconclusive. Reynolds and Warner (1988) showed significant reductions of glutamate in the hippocampus of DS subjects, with a tendency to lower levels in amygdala and caudate. The levels of GABA were diminished by 27% and 19% in the hippocampus and temporal cortex, respectively, but did not reach significance (Reynolds and Warner, 1988). Risser et al. (1997) found significantly reduced glutamate in the temporal cortex, but not in the frontal cortex. No regional differences were apparent in the control group, but a significantly lower level of glutamate was found in the parahippocampal gyrus than in the frontal cortex of DS subjects (Risser et al., 1997). In contrast, Seidl et al. (2001) find no significant differences in amino acid concentrations in adult DS subjects relative to controls. Recently, Whittle et al. (2007) showed significant reduction of GABA, but not glutamate in the frontal cortex of fetal subjects with DS. Additional studies of humans and of human tissue will be needed to document changes in neurotransmission and to examine them in the context of mouse model studies of the type reported herein. In providing evidence in a mouse model for region specific changes in synaptic structure and composition, we suggest that changes in neuronal circuits in people with DS will also be region-specific and that the pattern of changes can be used to elucidate important features of the underlying changes in the biology of cognitive and other circuits.

## Supplementary Material

Refer to Web version on PubMed Central for supplementary material.

## Acknowledgments

We thank the members of the Mobley Laboratory for critically reading the manuscript and for many helpful discussions.

Grant sponsor: National Institutes of Health; Grant numbers AG16999 and NS38869; Grant sponsor: The Hillblom Foundation; Grant sponsor: The Down Syndrome Research and Treatment Foundation.

## Literature Cited

Akerman CJ, Cline HT. 2007; Refining the roles of GABAergic signaling during neural circuit formation. Trends in neurosciences. 30 (8) :382–389. [PubMed: 17590449]

Belichenko PV, Kleschevnikov AM, Salehi A, Epstein CJ, Mobley WC. 2007; Synaptic and cognitive abnormalities in mouse models of Down syndrome: exploring genotype-phenotype relationships. The Journal of comparative neurology. 504 (4) :329–345. [PubMed: 17663443]

Belichenko PV, Masliah E, Kleschevnikov AM, Villar AJ, Epstein CJ, Salehi A, Mobley WC. 2004; Synaptic structural abnormalities in the Ts65Dn mouse model of Down Syndrome. The Journal of comparative neurology. 480 (3) :281–298. [PubMed: 15515178]

Bellocchio EE, Reimer RJ, Fremeau RT Jr, Edwards RH. 2000; Uptake of glutamate into synaptic vesicles by an inorganic phosphate transporter. Science (New York, NY). 289 (5481) :957–960.

Benes FM, Berretta S. 2001; GABAergic interneurons: implications for understanding schizophrenia and bipolar disorder. Neuropsychopharmacology. 25 (1) :1–27. [PubMed: 11377916]

Casanova MF, Walker LC, Whitehouse PJ, Price DL. 1985; Abnormalities of the nucleus basalis in Down's syndrome. Annals of neurology. 18 (3) :310–313. [PubMed: 2932050]

Chaudhry FA, Reimer RJ, Bellocchio EE, Danbolt NC, Osen KK, Edwards RH, Storm-Mathisen J. 1998; The vesicular GABA transporter, VGAT, localizes to synaptic vesicles in sets of glycinergic as well as GABAergic neurons. J Neurosci. 18 (23) :9733–9750. [PubMed: 9822734]

Chen R. 2004; Interactions between inhibitory and excitatory circuits in the human motor cortex. Experimental brain research Experimentelle Hirnforschung. 154 (1) :1–10. [PubMed: 14579004]

Chih B, Engelman H, Scheiffele P. 2005; Control of excitatory and inhibitory synapse formation by neuroligins. Science (New York, NY). 307 (5713) :1324–1328.

Demas GE, Nelson RJ, Krueger BK, Yarowsky PJ. 1998; Impaired spatial working and reference memory in segmental trisomy (Ts65Dn) mice. Behavioural brain research. 90 (2) :199–201. [PubMed: 9521551]

Escorihuela RM, Vallina IF, Martinez-Cue C, Baamonde C, Dierssen M, Tobena A, Florez J, Fernandez-Teruel A. 1998; Impaired short- and long-term memory in Ts65Dn mice, a model for Down syndrome. Neuroscience letters. 247 (2-3) :171–174. [PubMed: 9655620]

Fritschy JM, Meskenaite V, Weinmann O, Honer M, Benke D, Mohler H. 1999; GABAB-receptor splice variants GB1a and GB1b in rat brain: developmental regulation, cellular distribution and extrasynaptic localization. The European journal of neuroscience. 11 (3) :761–768. [PubMed: 10103070]

Galdzicki Z, Siarey R, Pearce R, Stoll J, Rapoport SI. 2001; On the cause of mental retardation in Down syndrome: extrapolation from full and segmental trisomy 16 mouse models. Brain research. 35 (2) :115–145. [PubMed: 11336779]

Gray EG. 1959; Electron microscopy of synaptic contacts on dendrite spines of the cerebral cortex. Nature. 183 (4675) :1592–1593. [PubMed: 13666826]

Greger IH, Ziff EB, Penn AC. 2007; Molecular determinants of AMPA receptor subunit assembly. Trends in neurosciences. 30 (8) :407–416. [PubMed: 17629578]

Hensch TK, Fagiolini M. 2005; Excitatory-inhibitory balance and critical period plasticity in developing visual cortex. Progress in brain research. 147 :115–124. [PubMed: 15581701]

Isaac JT, Ashby M, McBain CJ. 2007; The role of the GluR2 subunit in AMPA receptor function and synaptic plasticity. Neuron. 54 (6) :859–871. [PubMed: 17582328]

Kleschevnikov AM, Belichenko PV, Villar AJ, Epstein CJ, Malenka RC, Mobley WC. 2004; Hippocampal long-term potentiation suppressed by increased inhibition in the Ts65Dn mouse, a genetic model of Down syndrome. J Neurosci. 24 (37) :8153–8160. [PubMed: 15371516]

Kralic JE, Sidler C, Parpan F, Homanics GE, Morrow AL, Fritschy JM. 2006; Compensatory alteration of inhibitory synaptic circuits in cerebellum and thalamus of gamma-aminobutyric acid type A receptor alpha1 subunit knockout mice. The Journal of comparative neurology. 495 (4) :408–421. [PubMed: 16485284]

Kurt MA, Davies DC, Kidd M, Dierssen M, Florez J. 2000; Synaptic deficit in the temporal cortex of partial trisomy 16 (Ts65Dn) mice. Brain Res. 858 (1) :191–197. [PubMed: 10700614]

Luscher B, Keller CA. 2004; Regulation of GABAA receptor trafficking, channel activity, and functional plasticity of inhibitory synapses. Pharmacology & therapeutics. 102 (3) :195–221. [PubMed: 15246246]

Mann DM, Yates PO, Marcyniuk B, Ravindra CR. 1985; Pathological evidence for neurotransmitter deficits in Down's syndrome of middle age. Journal of mental deficiency research. 29 (Pt 2) :125–135. [PubMed: 2411933]

Marsden KC, Beattie JB, Friedenthal J, Carroll RC. 2007; NMDA receptor activation potentiates inhibitory transmission through GABA receptor-associated protein-dependent exocytosis of GABA(A) receptors. J Neurosci. 27 (52) :14326–14337. [PubMed: 18160640]

Meier J, Grantyn R. 2004; A gephyrin-related mechanism restraining glycine receptor anchoring at GABAergic synapses. J Neurosci. 24 (6) :1398–1405. [PubMed: 14960612]

Reeves RH, Irving NG, Moran TH, Wohn A, Kitt C, Sisodia SS, Schmidt C, Bronson RT, Davisson MT. 1995; A mouse model for Down syndrome exhibits learning and behaviour deficits. Nature genetics. 11 (2) :177–184. [PubMed: 7550346]

Reynolds GP, Warner CE. 1988; Amino acid neurotransmitter deficits in adult Down's syndrome brain tissue. Neuroscience letters. 94 (1-2) :224–227. [PubMed: 2907377]

Rippon G, Brock J, Brown C, Boucher J. 2007; Disordered connectivity in the autistic brain: challenges for the “new psychophysiology”. Int J Psychophysiol. 63 (2) :164–172. [PubMed: 16820239]

Risser D, Lubec G, Cairns N, Herrera-Marschitz M. 1997; Excitatory amino acids and monoamines in parahippocampal gyrus and frontal cortical pole of adults with Down syndrome. Life sciences. 60 (15) :1231–1237. [PubMed: 9096240]

Rubenstein JL, Merzenich MM. 2003; Model of autism: increased ratio of excitation/inhibition in key neural systems. Genes, brain, and behavior. 2 (5) :255–267.

Sago H, Carlson EJ, Smith DJ, Rubin EM, Crnic LS, Huang TT, Epstein CJ. 2000; Genetic dissection of region associated with behavioral abnormalities in mouse models for Down syndrome. Pediatric research. 48 (5) :606–613. [PubMed: 11044479]

Salehi A, Faizi M, Belichenko PV, Mobley WC. 2007; Using mouse models to explore genotype-phenotype relationship in Down syndrome. Mental retardation and developmental disabilities research reviews. 13 (3) :207–214. [PubMed: 17910089]

Seidl R, Cairns N, Singewald N, Kaehler ST, Lubec G. 2001; Differences between GABA levels in Alzheimer's disease and Down syndrome with Alzheimer-like neuropathology. Naunyn-Schmiedeberg's archives of pharmacology. 363 (2) :139–145.

Siarey RJ, Carlson EJ, Epstein CJ, Balbo A, Rapoport SI, Galdzicki Z. 1999; Increased synaptic depression in the Ts65Dn mouse, a model for mental retardation in Down syndrome. Neuropharmacology. 38 (12) :1917–1920. [PubMed: 10608287]

Siarey RJ, Stoll J, Rapoport SI, Galdzicki Z. 1997; Altered long-term potentiation in the young and old Ts65Dn mouse, a model for Down Syndrome. Neuropharmacology. 36 (11-12) :1549–1554. [PubMed: 9517425]

Trevelyan AJ, Watkinson O. 2005; Does inhibition balance excitation in neocortex? Progress in biophysics and molecular biology. 87 (1) :109–143. [PubMed: 15471593]

Wang H, Olsen RW. 2000; Binding of the GABA(A) receptor-associated protein (GABARAP) to microtubules and microfilaments suggests involvement of the cytoskeleton in GABARAPGABA(A) receptor interaction. Journal of neurochemistry. 75 (2) :644–655. [PubMed: 10899939]

Whittle N, Sartori SB, Dierssen M, Lubec G, Singewald N. 2007; Fetal Down syndrome brains exhibit aberrant levels of neurotransmitters critical for normal brain development. Pediatrics. 120 (6) :e1465–1471. [PubMed: 17998315]

Zold CL, Larramendy C, Riquelme LA, Murer MG. 2007; Distinct changes in evoked and resting globus pallidus activity in early and late Parkinson's disease experimental models. The European journal of neuroscience. 26 (5) :1267–1279. [PubMed: 17767504]

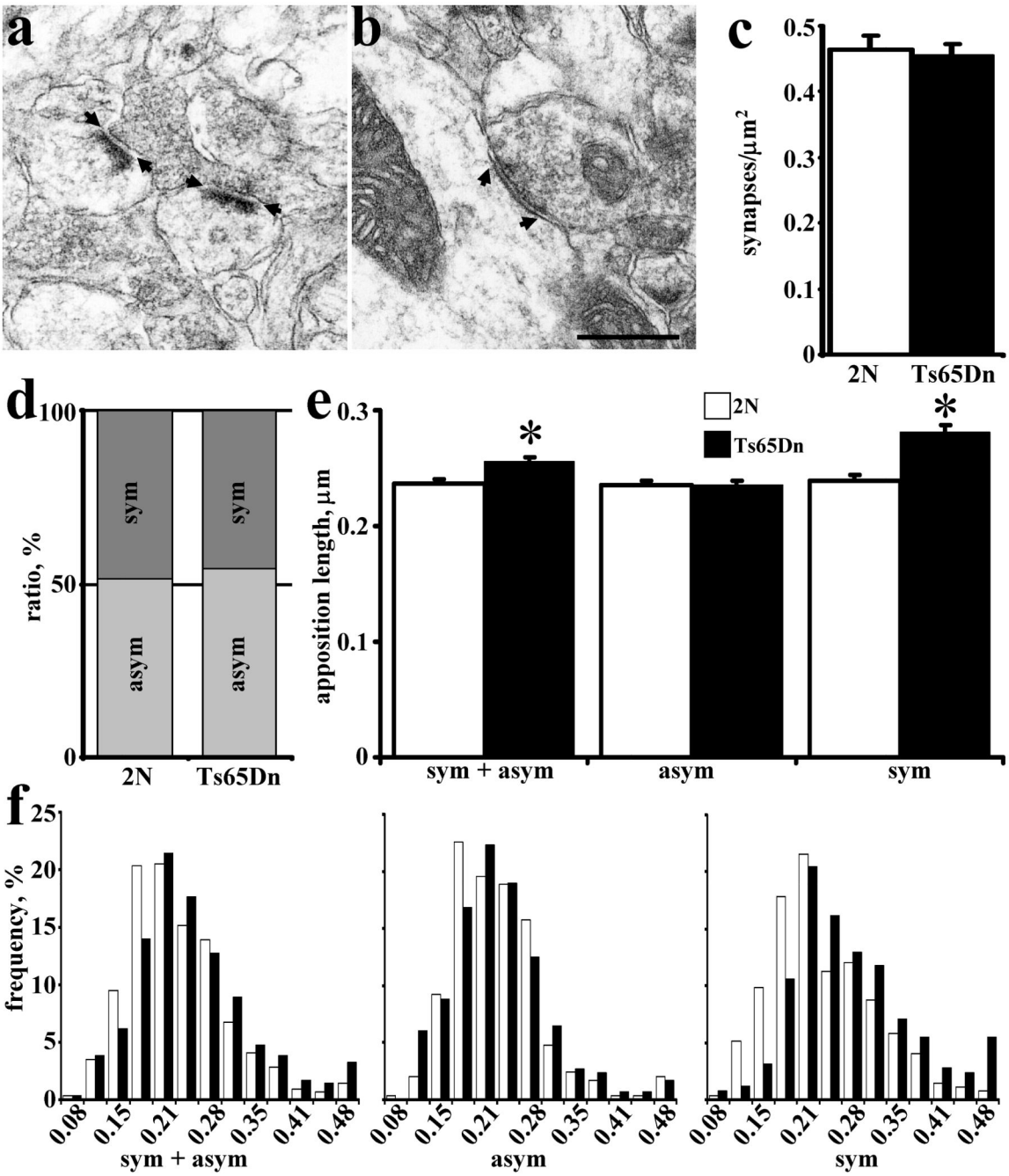


**Fig. 1.**

Quantitative analysis of EM images in molecular layer of fascia dentata. EM image of asymmetric (**a**) and symmetric (**b**) synapses; arrows denote the synaptic apposition measured. The area density of all synapses (**c**) and ratio of symmetric/asymmetric synapses (**d**) in 2N and Ts65Dn mice. The mean synaptic apposition length of all synapses combined and asymmetric or symmetric synapses separated (**e**) and their frequency distribution (**f**). Results are mean ± SEM. Number of mice examined: 2N = 4, Ts65Dn = 4. **P* < 0.05, significantly different from 2N mice. Scale bar = 0.5 µm.

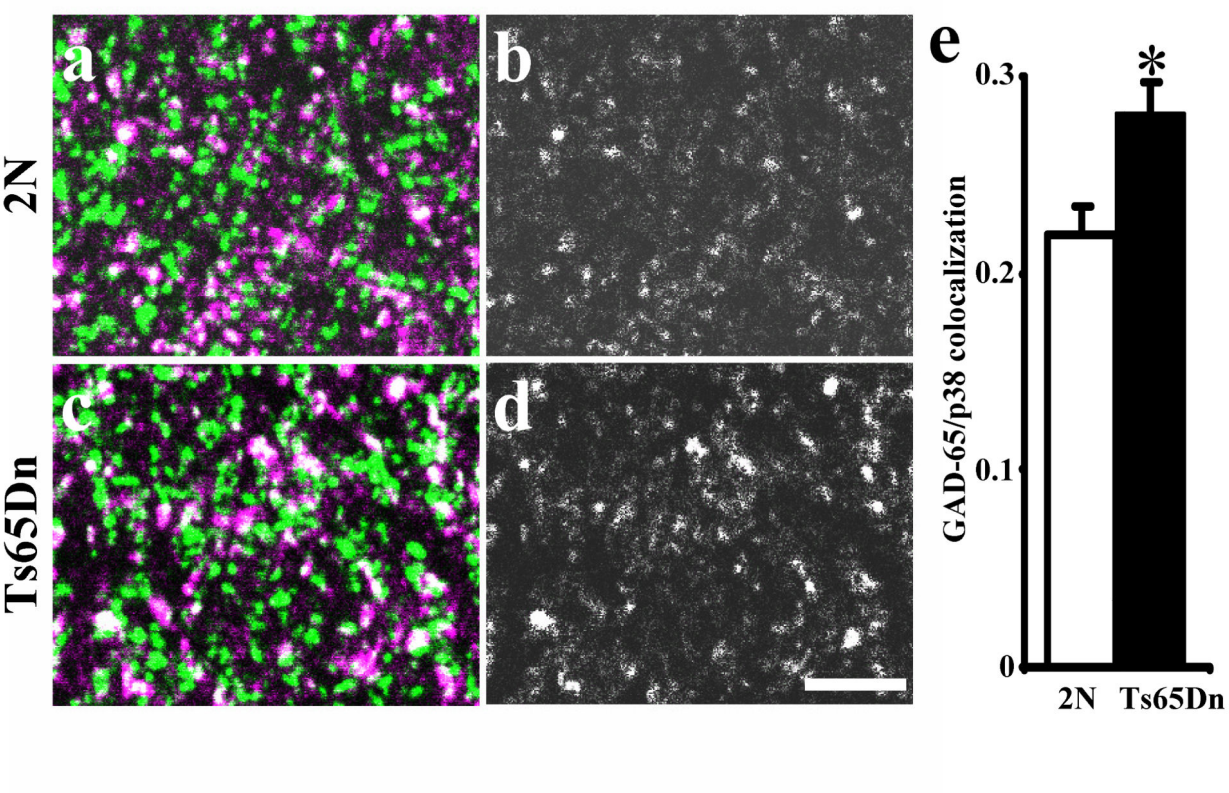


**Fig. 2.**

Colocalization of synaptophysin (p38, green) and GAD65 (magenta) in the middle molecular layer of fascia dentata in 3 months old 2N (**a, b**) and Ts65Dn (**c, d**) mice. **b** and **d** represent only colocalization (white) between these two markers. Note increase GAD65 to p38 colocalization in Ts65Dn (**d**) vs. 2N (**b**) mice. In average, coefficient of colocalization of GAD65/p38-IR was ~30% higher in molecular layer of fascia dentata in Ts65Dn vs. 2N mice (**e**). Results are mean ± SEM. Number of mice examined: 2N = 3, Ts65Dn = 3. **P* < 0.05, significantly different from 2N mice. Scale bar = 5 μm.

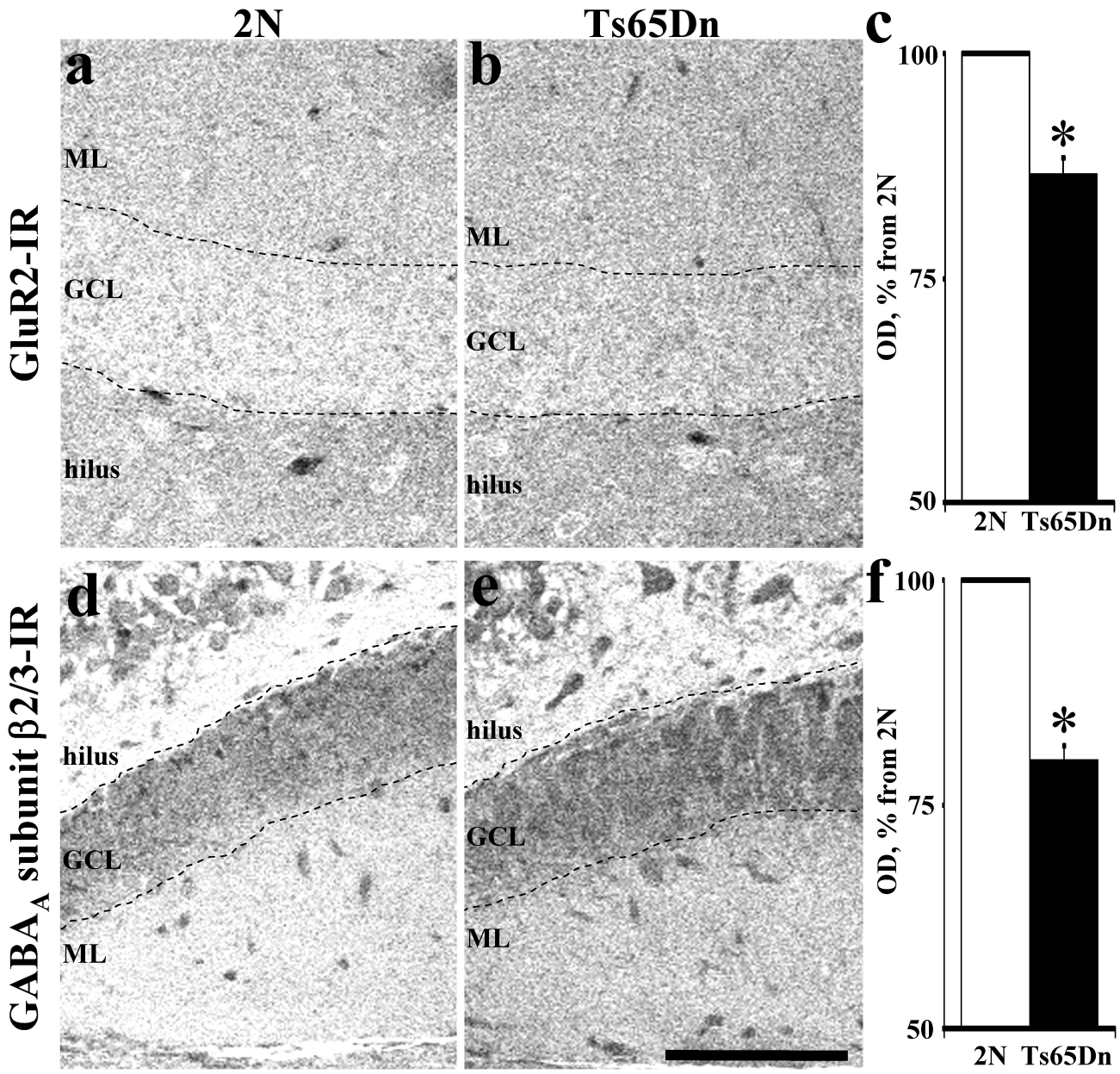


**Fig. 3.**

Confocal images of GluR2-IR (**a, b**) and $GABA_A$ subunit β2/3-IR (**c, d**) from hippocampus in 3 months old 2N and Ts65Dn mice. Note decreased optical density of GluR2-IR and $GABA_A$ subunit β2/3-IR in Ts65Dn as compared to 2N mice. In average, optical densities were ~13% lover for GluR2-IR (**c**) and ~20% lover for $GABA_A$ subunit β2/3-IR (**f**) in fascia dentata in Ts65Dn vs. 2N mice. Results are mean ± SEM. Number of mice examined: 2N = 6, Ts65Dn = 5. **P* < 0.05, significantly different from 2N mice. GCL – granular cell layer, ML – molecular layer. Scale bar = 100 μm.

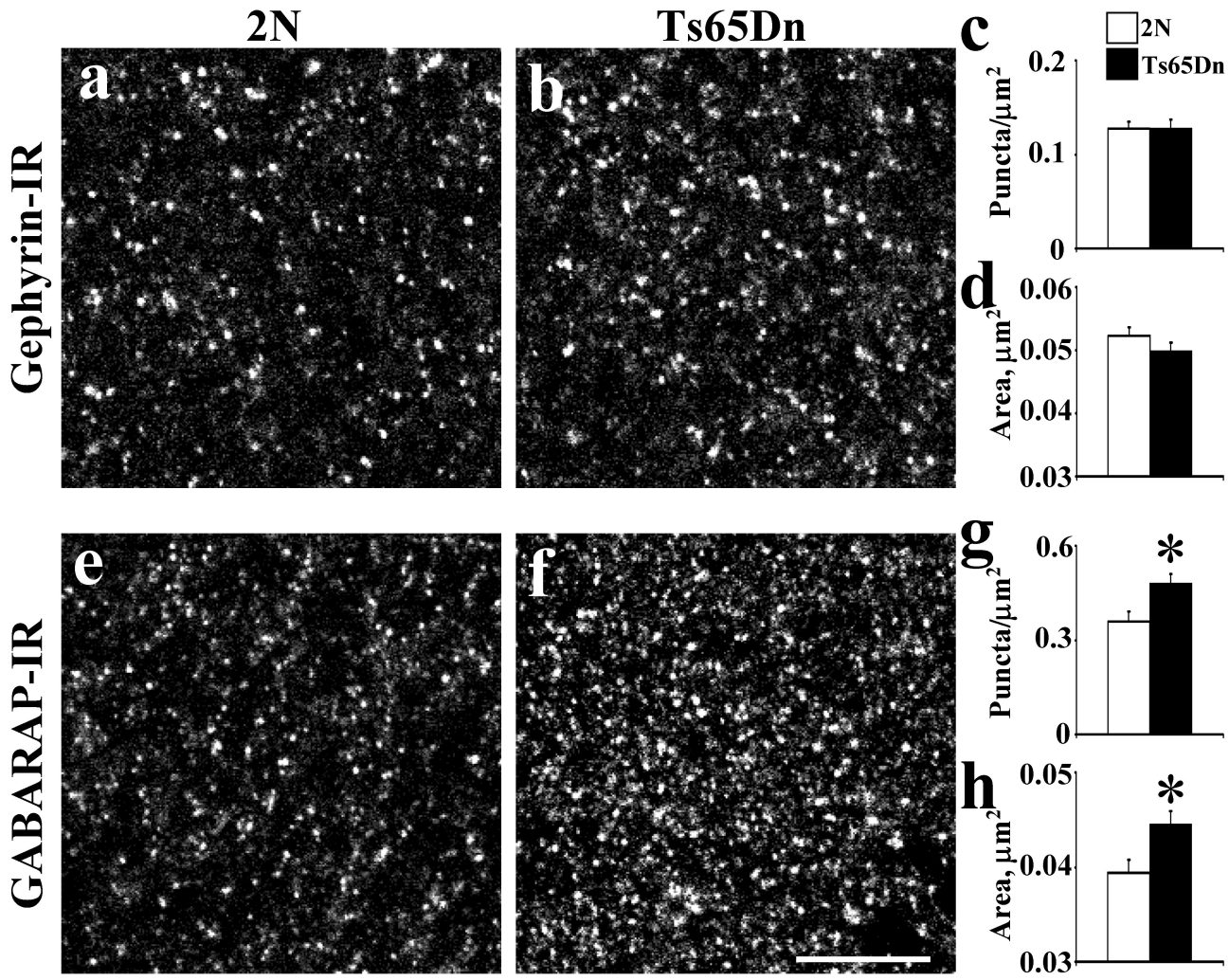


**Fig. 4.**

Quantitative analysis of the distribution of gephyrin-IR (**a-d**) and GABARAP-IR (**e-h**) in the fascia dentata in 2N and Ts65Dn mice at 3 months old. The density (**c, g**) and area of individual puncta (**d, h**) with intensity value above a background threshold were calculated. Results are mean ± SEM. Number of mice examined: 2N = 6, Ts65Dn = 6. **P* < 0.05, significantly different from 2N mice. Scale bar = 10 μm.

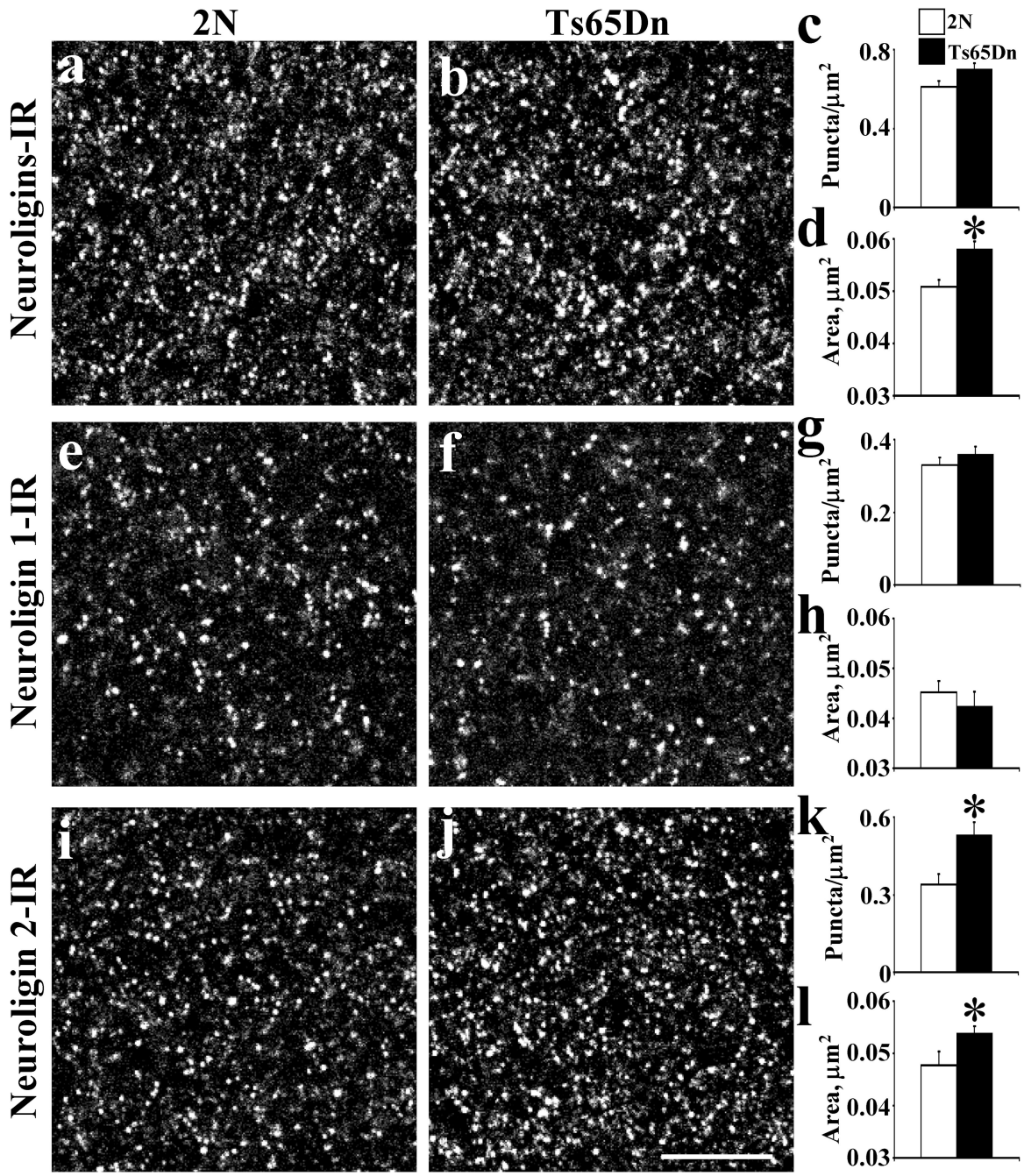


**Fig. 5.**

Quantitative analysis of the distribution of neuroligins-IR (a-d), neuroligin 1-IR (e-h) and neuroligin 2-IR (i-l) in the fascia dentata in 2N and Ts65Dn mice at 3 months old. The density (**c, g, k**) and area of individual puncta (**d, h, l**) with intensity value above a background threshold were calculated. Results are mean ± SEM. Number of mice examined: 2N = 6, Ts65Dn = 6. **P* < 0.05, significantly different from 2N mice. Scale bar = 10 μm.

## Table 1

### Primary Antibodies

| Name of antibody | Manufacturer | Catalog and lot no. | Species | Exact structure of immunizingantigen |
|---|---|---|---|---|
| Anti-synaptophysin (p38) | Boehringer, Germany | 902314, lot 12530025-03 | Mouse | Vesicular fraction of bovine brain |
| Anti-glutamate decarboxylase 65 (GAD65) | Chemicon, USA | AB5082, lot 24051184 | Rabbit | Human GAD65 from baculovirus infected cells |
| Anti-vesicular GABA transporter (VGAT) | Chaudhry et al., 1998 | | Rabbit | GST fusion protein containing N-terminal 99 amino acids of rat VGAT |
| Anti-vesicular glutamate transporter 1 (VGLUT1) | Bellocchio et al., 1998 | | Rabbit | GST fusion protein containing last 68 amino acids (residues 493-560) of rat specific Na+ - dependent inorganic phosphate transporter |
| Anti-glutamate receptor 2 (GluR2), clone 6C4 | Chemicon, USA | MAB397, lot 22041088 | Mouse | Recombinant fusion protein TrpE-GluR2 (N-terminal portion, amino acid 175-430 of rat GluR2 |
| Anti-glutamate receptor 1 (GluR1) | Chemicon, USA | AB1504, lot 22090149 | Rabbit | Carboxy terminus peptide of rat GluR1 conjugated to BSA with glutaraldehyde (SHSSGMPLGATGL) |
| Anti-$GABA_A$ receptor β2/3, clone 62-3G1 | Upstate, USA | 05-474, lot 17280 | Mouse | Affinity-purified $GABA_A$ receptor isolated from bovine brain |
| Anti-$GABA_A$ receptor α1 | Upstate, USA | 06-868, lot 22589 | Rabbit | Synthetic peptide (QPSQDELKDNTTVFT-C) corresponding to amino acids 1-15 of the mature rat $GABA_A$ receptor α1 subunit containing a cysteine at the C-terminus for linkage to a carrier protein |
| Anti-$GABA_B$ receptor R1 | Chemicon, USA | AB5850, lot 23050396 | Rabbit | Amino acid 33-54 of the rat $GABA_B$ R1 protein (PHLPRPHPRVPPHPSSERRAVY) |
| Anti-$GABA_B$ receptor R2, a.a. 42-54 rat | Chemicon, USA | AB5848, lot 23010140 | Rabbit | Amino acids 42-54 of the rat 105 kDa $GABA_B$ R2 protein |
| Anti-neuroligin, clone 4F9 | Synaptic Systems, Germany | 129011, lot 129011/10 | Mouse | Recombinant protein containing the extracellular sequence (residues 1-695) of neuroligin 1 |
| Anti-neuroligin 1, clone 4C12 | Synaptic Systems, Germany | 129111, lot 129111/1 | Mouse | Recombinant protein containing the extracellular sequence (residues 1-695) of neuroligin 1 |
| Anti-neuroligin 2 (R-16) | Santa Cruz, USA | sc-14089, lot k1403 | Goat | Amino acid peptide (KGGPLLPTAGRELPPEE) of neuroligin 2 of rat origin |
| Anti-GABARAP | Abcam, USA | ab1398-50, lot 201420 | Rabbit | Synthetic peptide (RSEGEKIRKKYPDRVPV) corresponding to amino acids 15-31 of human gabarap |
| Anti-gephyrin, clone mAb7a (GlyR7a) | Synaptic Systems, Germany | 147011, lot 147011/15 | Mouse | Purified rat gephyrin |

**Table 2**

**Quantitative Analysis of GluR2 and GluR1 Receptors in 3 and 8 Months Old Ts65Dn and 2N Mice Hippocampus[1]**

| GluR receptor subunit | GluR2 | | | | | GluR1 | | | | | | |
|---|---|---|---|---|---|---|---|---|---|---|---|---|
| Age of mice | 3 months old | | 8 months old | | 3/8 months ratio | 3 months old | | 8 months old | | 3/8 months ratio | GluR2/GluR1 ratio at 3 months | GluR2/GluR1 ratio at 8 months |
| Statistical data | % from 2N | *P* value | % from 2N | *P* value | | % from 2N | *P* value | % from 2N | *P* value | | | |
| Fascia dentata, inferior blade | | | | | | | | | | | | |
| Inner ML | **82.4 ± 3.6** | 0.004 | 81.3 ± 8.2 | 0.089 | 1.01 | 89.1 ± 5.5 | 0.167 | 82.6 ± 5.7 | 0.054 | 1.08 | 0.92 | 0.98 |
| Middle ML | **80.4 ± 4.8** | 0.013 | 92.0 ± 17.1 | 0.337 | 0.88 | 85.7 ± 5.4 | 0.107 | 85.9 ± 5.5 | 0.115 | 1.00 | 0.94 | 1.07 |
| Outer ML | **72.6 ± 5.1** | 0.005 | 86.7 ± 18.0 | 0.256 | **0.84** | **83.4 ± 4.2** | 0.044 | 83.5 ± 6.6 | 0.065 | 1.00 | **0.87** | 1.04 |
| Granular layer | **84.1 ± 4.0** | 0.005 | 91.8 ± 8.8 | 0.257 | 0.92 | 86.4 ± 6.9 | 0.136 | 84.3 ± 10.5 | 0.148 | 1.02 | 0.97 | 1.09 |
| Fascia dentata, superior blade | | | | | | | | | | | | |
| Inner ML | **82.6 ± 3.5** | 0.001 | **73.8 ± 4.3** | 0.004 | **1.12** | 87.1 ± 6.1 | 0.124 | 85.0 ± 2.7 | 0.074 | 1.03 | 0.95 | **0.87** |
| Middle ML | **91.1 ± 4.5** | 0.024 | **75.1 ± 3.2** | 0.009 | **1.21** | 88.9 ± 8.4 | 0.196 | 86.8 ± 4.2 | 0.147 | 1.02 | 1.03 | **0.87** |
| Outer ML | 90.9 ± 9.3 | 0.098 | **75.9 ± 4.7** | 0.009 | **1.20** | 90.9 ± 9.2 | 0.267 | 103.0 ± 7.5 | 0.430 | 0.88 | 1.00 | **0.74** |
| Granular layer | **86.4 ± 2.8** | 0.034 | 90.8 ± 10.9 | 0.246 | 0.95 | 88.0 ± 9.4 | 0.137 | 91.8 ± 8.7 | 0.265 | 0.96 | 0.98 | 0.99 |
| Hilus, neuropil | **87.0 ± 3.0** | 0.005 | 86.2 ± 3.0 | 0.090 | 1.01 | 87.5 ± 5.6 | 0.053 | **76.5 ± 5.2** | 0.040 | **1.14** | 0.99 | **1.13** |
| CA1 area of hippocampus | | | | | | | | | | | | |
| Stratum oriens | 93.1 ± 4.8 | 0.074 | **79.0 ± 6.1** | 0.035 | **1.18** | 90.1 ± 2.6 | 0.097 | 90.0 ± 6.2 | 0.182 | 1.00 | 1.03 | 0.88 |
| Stratum pyramidale | 96.0 ± 5.7 | 0.233 | **80.5 ± 11.0** | 0.040 | **1.19** | 91.7 ± 6.4 | 0.221 | 82.4 ± 5.8 | 0.072 | 1.11 | 1.05 | 0.98 |
| Stratum radiatum | 93.3 ± 5.8 | 0.140 | **76.1 ± 3.8** | 0.045 | **1.23** | 87.0 ± 3.3 | 0.073 | 87.0 ± 6.3 | 0.100 | 1.00 | 1.07 | **0.87** |
| Stratum lacunosum moleculare | **85.3 ± 2.6** | 0.020 | **70.7 ± 5.6** | 0.007 | **1.21** | **82.4 ± 3.7** | 0.029 | **79.9 ± 4.8** | 0.018 | 1.03 | 1.04 | 0.88 |

[1]The number of mice used was as follows: 2N/Ts65Dn = 3/3 for 3 months old and 3/4 for 8 months old. ML, molecular layer.

Bold type face represents significant difference of studied parameters.

**Table 3**

**Quantitative Analysis of $GABA_A$ Receptor Subunits β2/3 and α1 in 3 and 8 Months Old Ts65Dn and 2N Mice Hippocampus[1]**

| $GABA_A$ receptor subunit | β2/3 | | | | | α1 | | | | | | |
|---|---|---|---|---|---|---|---|---|---|---|---|---|
| Age of mice | 3 months old | | 8 months old | | 3/8 months ratio | 3 months old | | 8 months old | | 3/8 months ratio | β2/3/α1 ratio at 3 months | β2/3/α1 ratio at 8 months |
| Statistical data | % from 2N | *P* value | % from 2N | *P* value | | % from 2N | *P* value | % from 2N | *P* value | | | |
| Fascia dentata, inferior blade | | | | | | | | | | | | |
| Inner ML | **75.1 ± 3.5** | 0.003 | 106.0 ± 14.2 | 0.458 | **0.71** | 93.9 ± 4.7 | 0.165 | 109.1 ± 6.9 | 0.356 | **0.86** | **0.80** | 0.97 |
| Middle ML | **75.8 ± 2.7** | 0.001 | 105.4 ± 15.9 | 0.444 | **0.72** | 96.5 ± 4.2 | 0.294 | 112.6 ± 5.2 | 0.265 | **0.86** | **0.79** | 0.94 |
| Outer ML | **67.8 ± 2.4** | 0.001 | 100.7 ± 17.1 | 0.279 | **0.67** | 97.3 ± 4.6 | 0.314 | 110.1 ± 5.6 | 0.312 | 0.88 | **0.70** | 0.91 |
| Granular layer | **75.9 ± 4.6** | 0.040 | 116.2 ± 8.9 | 0.236 | **0.65** | 106.2 ± 10.3 | 0.111 | 104.6 ± 14.1 | 0.399 | 1.02 | **0.71** | 1.11 |
| Fascia dentata, superior blade | | | | | | | | | | | | |
| Inner ML | **82.4 ± 2.1** | 0.034 | 88.1 ± 10.5 | 0.160 | 0.94 | 95.6 ± 4.5 | 0.265 | 104.6 ± 16.2 | 0.382 | 0.91 | **0.86** | **0.84** |
| Middle ML | 84.7 ± 3.7 | 0.054 | 97.9 ± 13.2 | 0.295 | **0.86** | 94.3 ± 4.1 | 0.220 | 97.7 ± 15.8 | 0.280 | 0.97 | 0.90 | 1.00 |
| Outer ML | 82.1 ± 3.3 | 0.059 | 95.6 ± 12.1 | 0.280 | **0.86** | 95.3 ± 5.1 | 0.214 | 98.8 ± 12.5 | 0.324 | 0.96 | **0.86** | 0.97 |
| Granular layer | 81.8 ± 4.3 | 0.082 | 113.4 ± 13.1 | 0.379 | **0.72** | 114.1 ± 7.6 | 0.068 | 101.7 ± 19.5 | 0.269 | 1.12 | **0.72** | 1.11 |
| Hilus, neuropil | **86.7 ± 1.5** | 0.001 | 90.1 ± 8.3 | 0.117 | 0.96 | 93.7 ± 5.9 | 0.121 | 97.5 ± 11.0 | 0.339 | 0.96 | 0.93 | 0.92 |
| CA1 area of hippocampus | | | | | | | | | | | | |
| Stratum oriens | **87.2 ± 1.4** | 0.002 | 86.6 ± 6.5 | 0.054 | 1.01 | 92.2 ± 3.3 | 0.101 | 94.4 ± 8.4 | 0.282 | 0.98 | 0.95 | 0.92 |
| Stratum pyramidale | **78.2 ± 3.1** | 0.001 | 109.5 ± 13.5 | 0.472 | **0.71** | 102.6 ± 9.6 | 0.404 | 88.2 ± 16.3 | 0.173 | **1.16** | **0.76** | **1.24** |
| Stratum radiatum | **85.9 ± 1.8** | 0.006 | 94.1 ± 11.5 | 0.211 | 0.91 | 92.5 ± 6.1 | 0.101 | 84.9 ± 7.1 | 0.179 | 1.09 | 0.93 | 1.11 |
| Stratum lacunosum moleculare | **74.7 ± 2.6** | 0.005 | 85.0 ± 10.6 | 0.118 | 0.88 | **85.0 ± 4.2** | 0.021 | 82.1 ± 7.5 | 0.125 | 1.04 | 0.88 | 1.04 |

[1]The number of mice used was as follows: 2N/Ts65Dn = 3/3 for 3 months old and 3/4 for 8 months old. ML, molecular layer.

Bold type face represents significant difference of studied parameters.

**Table 4**

**Quantitative Analysis of $GABA_B$ R1 and R2 Receptors in 3 and 11.5 Months Old Ts65Dn and 2N Mice Hippocampus[1]**

| $GABA_B$ receptor subunit | R1 | | | | | R2 | | | | | | |
|---|---|---|---|---|---|---|---|---|---|---|---|---|
| Age of mice | 3 months old | | 11.5 months old | | 3/11.5 months ratio | 3 months old | | 11.5 months old | | 3/11.5 months ratio | R1/R2 ratio at 3 months | R1/R2 ratio at 11.5 months |
| Statistical data | % from 2N | *P* value | % from 2N | *P* value | | % from 2N | *P* value | % from 2N | *P* value | | | |
| Fascia dentata, inferior blade | | | | | | | | | | | | |
| Inner ML | 90.9 ± 5.5 | 0.186 | 86.5 ± 4.2 | 0.1178 | 1.05 | 102.0 ± 2.9 | 0.36 | 100.4 ± 7.1 | 0.45 | 1.02 | 0.89 | **0.86** |
| Middle ML | 95.5 ± 4.7 | 0.310 | 86.8 ± 4.3 | 0.1823 | 1.10 | 104.8 ± 3.0 | 0.21 | 99.0 ± 5.6 | 0.40 | 1.06 | 0.91 | 0.88 |
| Outer ML | 87.2 ± 4.5 | 0.136 | 96.5 ± 5.9 | 0.3816 | 0.90 | 97.9 ± 4.0 | 0.38 | 98.1 ± 3.4 | 0.43 | 1.00 | 0.89 | 0.98 |
| Granular layer | **86.3 ± 4.0** | 0.021 | 86.9 ± 3.9 | 0.0721 | 0.99 | 97.5 ± 3.7 | 0.26 | 100.5 ± 4.1 | 0.49 | 0.97 | 0.89 | **0.86** |
| Fascia dentata, superior blade | | | | | | | | | | | | |
| Inner ML | 95.8 ± 5.8 | 0.284 | **78.6 ± 2.0** | 0.0007 | **1.22** | 101.3 ± 3.1 | 0.39 | 101.2 ± 4.5 | 0.42 | 1.00 | 0.95 | **0.78** |
| Middle ML | 95.4 ± 3.7 | 0.175 | 85.3 ± 5.8 | 0.0569 | 1.12 | 107.5 ± 2.9 | 0.09 | 105.8 ± 3.7 | 0.25 | 1.02 | 0.89 | **0.81** |
| Outer ML | 94.3 ± 3.3 | 0.192 | **81.1 ± 2.1** | 0.0015 | **1.16** | 105.3 ± 4.1 | 0.21 | 96.7 ± 1.9 | 0.33 | 1.09 | 0.90 | **0.84** |
| Granular layer | 93.4 ± 3.5 | 0.216 | **75.6 ± 2.8** | 0.0011 | **1.24** | 99.8 ± 2.4 | 0.48 | 90.8 ± 5.8 | 0.17 | 1.10 | 0.94 | **0.83** |
| Hilus, neuropil | 79.9 ± 6.3 | 0.068 | **62.6 ± 2.4** | 0.0002 | **1.28** | 86.4 ± 10.4 | 0.11 | 89.5 ± 9.2 | 0.19 | 0.96 | 0.93 | **0.70** |
| CA1 area of hippocampus | | | | | | | | | | | | |
| Stratum oriens | 95.6 ± 3.2 | 0.285 | **81.3 ± 3.7** | 0.0141 | **1.17** | 101.5 ± 2.5 | 0.36 | 106.9 ± 6.2 | 0.19 | 0.95 | 0.94 | **0.76** |
| Stratum pyramidale | 92.6 ± 3.2 | 0.119 | **77.4 ± 6.5** | 0.0109 | **1.20** | 99.4 ± 1.0 | 0.41 | 97.7 ± 4.3 | 0.39 | 1.02 | 0.93 | **0.79** |
| Stratum radiatum | 100.9 ± 2.8 | 0.453 | **82.0 ± 4.3** | 0.0363 | **1.23** | 101.5 ± 2.5 | 0.40 | 91.7 ± 3.5 | 0.09 | 1.11 | 1.00 | 0.89 |
| Stratum lacunosum moleculare | 94.5 ± 3.2 | 0.202 | **66.4 ± 6.4** | 0.0053 | **1.42** | 95.1 ± 5.6 | 0.30 | 89.1 ± 5.7 | 0.13 | 1.07 | 0.99 | **0.74** |

[1]The number of mice used was as follows: 2N/Ts65Dn = 5/5 for each age. ML, molecular layer.

Bold type face represents significant difference of studied parameters